Observations of trapped and precipitating electrons in the auroral zone, and related effects in the ionospheric D-region.

J. K. Hargreaves[1,3], M. J. Birch[1,2], B. J. I. Bromage[1]

(1) Jeremiah Horrocks Institute for Astrophysics and Supercomputing,
University of Central Lancashire, UK.
(2) John Tyndall Institute for Nuclear Research, University of Central Lancashire, UK.
(3) Department of Communication Systems, Lancaster University, UK.

Abstract

This study investigates the relationship between the trapped and precipitated components of the >30 keV and >100 keV auroral electron flux measured by the polar orbiting environmental satellites (POES) which are in sun-synchronous orbits of 90 minutes period at an altitude of about 850 km. The data are restricted to selected over-passes of the Kilpisjärvi imaging riometer by the POES NOAA-12 and NOAA-14. The analysis of the data addresses the short-term variation of the fluxes, and the relation between the particle flux and the ionospheric radiowave absorption measured by the imaging riometer.

It is found that during each over-pass the precipitated flux varies more than the trapped, and the amount of variation is greatest in the morning sector and least at noon. The expectation that $(\text{absorption})^2 \propto$ flux holds more closely for the trapped than for the precipitated flux, an anomaly which may be explained in part if some of the electrons reaching 90 km are beyond the reception cone of the detector for precipitated particles. Empirical formulae are given for the relations between flux and absorption, and it is shown that the absorption may serve to estimate the diffusion parameter for >30 keV electrons.

1. Analysis of POES data at 2-seconds resolution: short-term variability

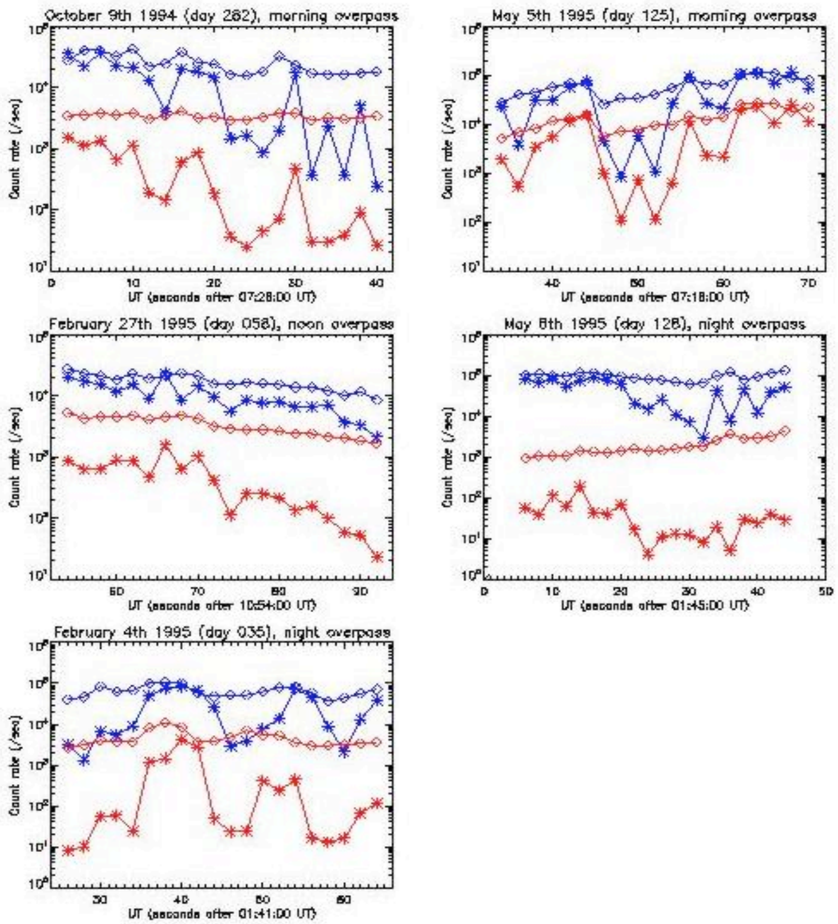

Figure 1: Variation with UT of trapped and precipitated count rates for both >30 keV and >100 keV detector channels, for selected passes during morning, noon and night (blue >30 keV; red >100 keV; asterisks = precipitated; diamonds = trapped)

Overpasses of POES satellites across a 240 km square centred on Kilpisjärvi, Finland (69.05^{O}N, 20.79^{O}E, L = 5.9) were selected for comparison with the radiowave absorption observed with the 38.2 MHz imaging riometer at that site. In the energy ranges >30 and >100 keV the electrons are counted for 1-second periods by the "0^{O}" and "90^{O}" telescopes alternately*. Thus the time resolution is 2 seconds in each case. During an overpass the number of samples taken was generally 18 to 20, giving a spatial resolution of about 12 km over the ground.

Samples of the count rate from the >30 keV and >100 keV counters at 0^{O} and 90^{O} are shown in Figure 1. It is noteworthy that the flux at 0^{O} is usually smaller than that at 90^{O} at the same energy, but the relative variations from point-to-point are considerably larger. The patterns of variation are similar for the >30 and >100 keV particles.

[*The two detectors are intended for the precipitating and trapped fluxes respectively, and in the auroral regions, on average, point at 17^{O} and 78^{O} to the magnetic field.]

The amount of variability depends on the time of day. Table 1 gives statistics of the maximum point-to-point change of precipitated (P) and trapped (T) flux (as a ratio) observed during each overpass, according to the 'morning' (≈ 08:30 LT), 'noon' (≈ 11:30 LT), and 'night' (≈ 02:30 LT) sectors and for energy ranges >30 and >100 keV. These groups include 31, 13 and 10 passes respectively.

LT group	P_{30}					P_{100}				
	No	Median ratio	% of values in the range			No	Median ratio	% of values in the range		
			≤10	10 - 100	>100			≤10	10 - 100	>100
Morning	31	35	16	68	16	31	25	22	61	16
Noon	13	2.7	100	0	0	12	4.5	92	8	0
Night	10	8.2	60	40	0	10	8.0	60	40	0

LT group	T_{30}			T_{100}		
	No	Median ratio	% of values ≤ 2	No	Median ratio	% of values ≤ 2
Morning	31	1.9	61	31	1.7	81
Noon	13	1.3	100	13	1.3	100
Night	10	1.8	60	10	1.6	60

Table 1: Statistical summary, showing the maximum change of precipitated and trapped flux from point-to-point (expressed as a ratio) observed during each overpass, divided according to time of day, energy, and whether precipitated or trapped.

The following conclusions are noted:

1. In general, the precipitated flux varies more than the trapped.

2. The maximum point-to-point changes in the morning group are generally large, 60-70% of values being between factors 10 and 100. The factor 100 was exceeded in 16% of the overpasses. The results are similar for >30 and >100 keV.

3. The relative variation of precipitated flux at night is smaller than in the morning group, the median being about 8 (which is 3 to 4 times smaller than in the morning).

4. The changes are smaller again at noon, when the median ratios for the precipitated particles are only 2 to 3 times those for the trapped component. Virtually all noon ratios are below 10, and at 30 keV they are below 5. This seems to indicate a remarkable change of character in only 3 hours of local time.

2. Relations between particle flux and radio absorption.

The imaging riometer at Kilpisjärvi measures the absorption of the cosmic radio noise at 38.2 MHz over a region of about 240 km north-south and east-west, assuming that the absorption occurs in the ionospheric D-region at altitude 90 km. Figure 2 shows the distribution of absorption (in decibels) obtained for the time of the overpass by NOAA-12 from 07:16:35 UT to 07:17:08 UT on day 125 (May 5th) of 1995. The projected track of the satellite is marked in black. An absorption value was then obtained by interpolation for each 2-second interval along the track. Figure 3 shows the variation in the absorption distribution from 07:14:30 UT to 07:19:00 UT at 30-second resolution. It is clear that most of the variation of absorption and particle flux was spatial rather than temporal.

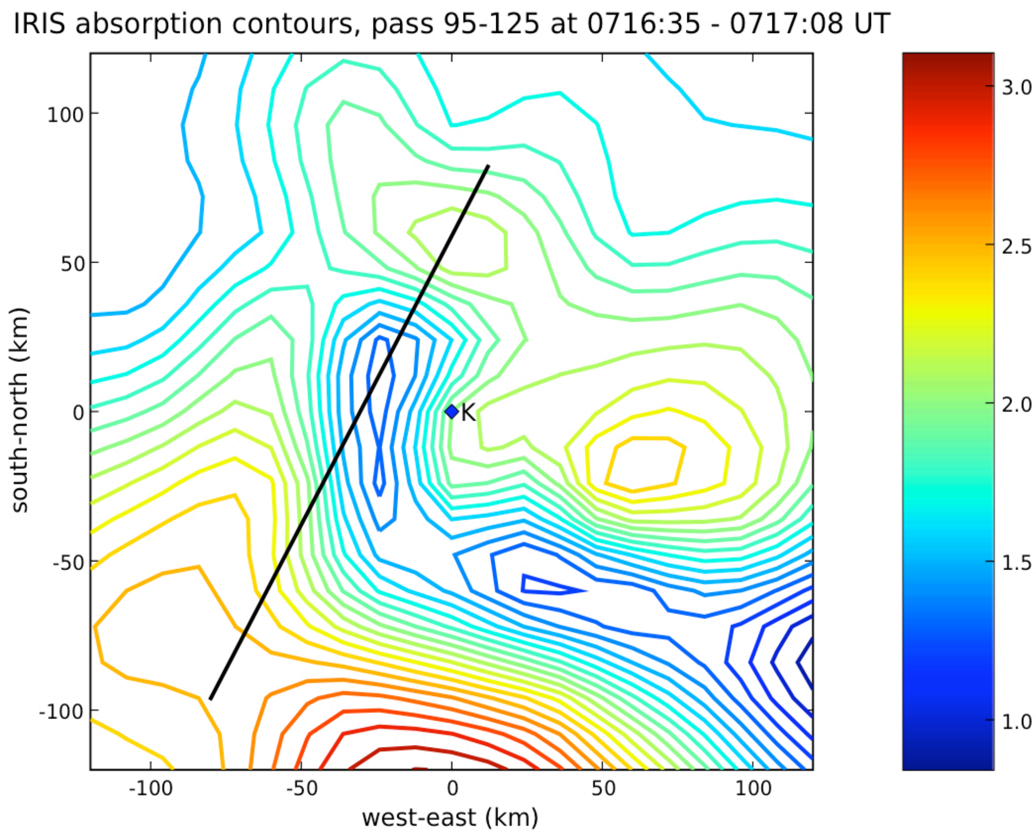

Figure 2: The distribution of absorption (in dB) at 90 km altitude for the time of the overpass by NOAA-12 (07:16:35 to 07:17:08 UT on May 5th 1995), observed using the Kilpisjärvi imaging riometer (satellite track shown in black).

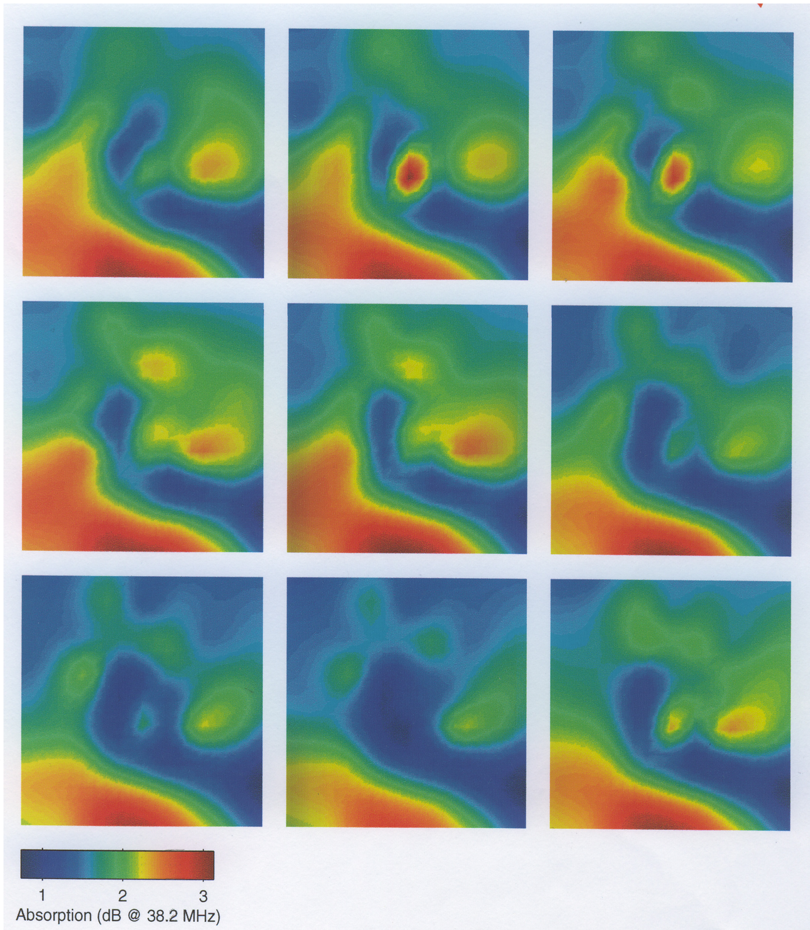

Figure 3: Change in absorption from 07:14:30 UT to 07:19:00 UT (30-second resolution). Each panel covers the same area as Figure 2.

The continuity equation appropriate to the D-region, $q = \alpha_e N_e^2$ (where q is the ion production rate, α_e is the effective recombination coefficient, and N_e is the equilibrium electron density), indicates that the square of the absorption (in decibels) should be proportional to the flux of incoming ionising particles. Figure 4(a) compares the >30 keV fluxes, both trapped and precipitated, with the square of the 38.2 MHz absorption from the imaging riometer, for the overpass in Figure 2. There is an obvious similarity, but, remarkably, the $(\text{absorption})^2$ agrees most closely not with the 0^O (precipitated) flux but with that observed with the 90^O (trapped) detector. The same result is obtained for the other overpasses having significant radio absorption; that on day 35 (February 4th) is shown in Figure 4(b).

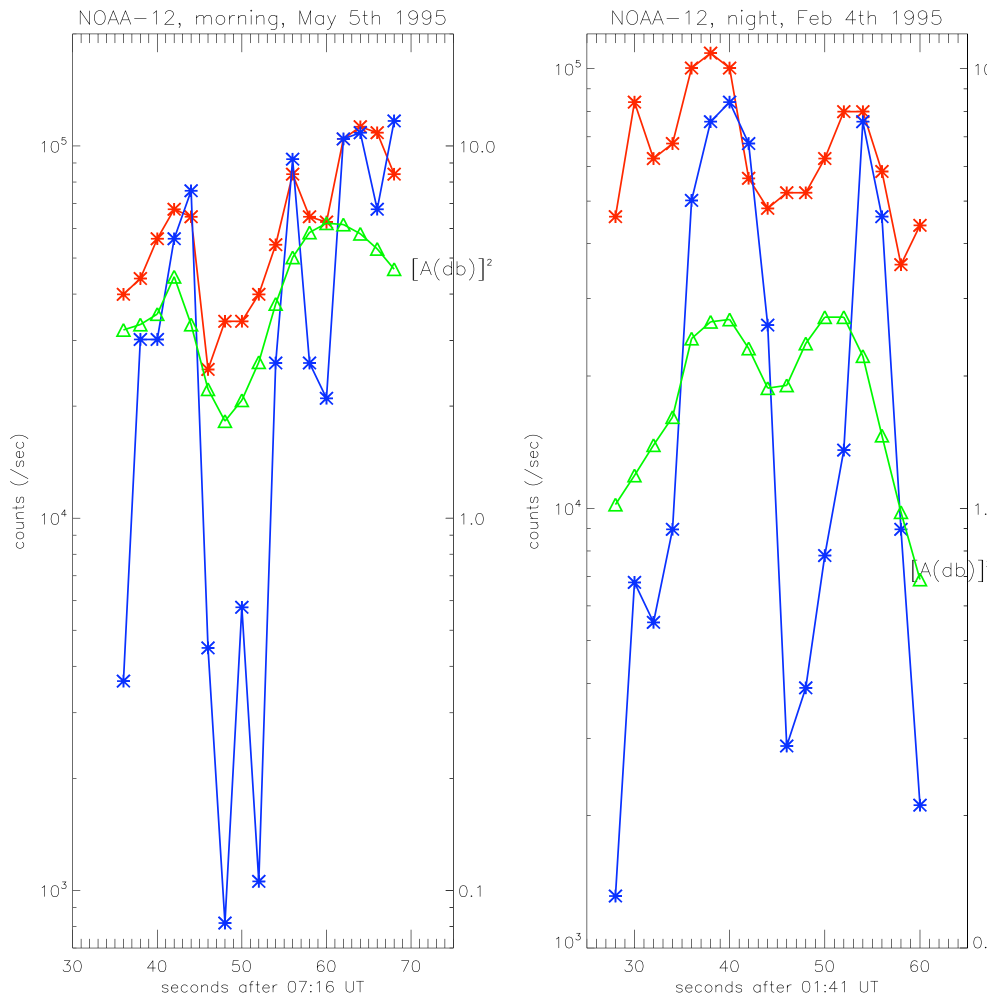

Figure 4: Comparison of $[A(db)]^2$ (green) with both precipitated (blue) and trapped (red) count rates at 30 keV, for passes by NOAA-12 on May 5th (day 125) and February 4th (day 35) in the morning and night sectors, respectively.

The relationships are summarised statistically in Figures 5 and 6, which plot absorption (in dB) against trapped or precipitated count rate (respectively) for 8 overpasses at times of significant absorption (0.3 to 2.5 dB). Of these two plots, only Figure 5 is close to the expected behaviour ($A^2 \propto$ flux).

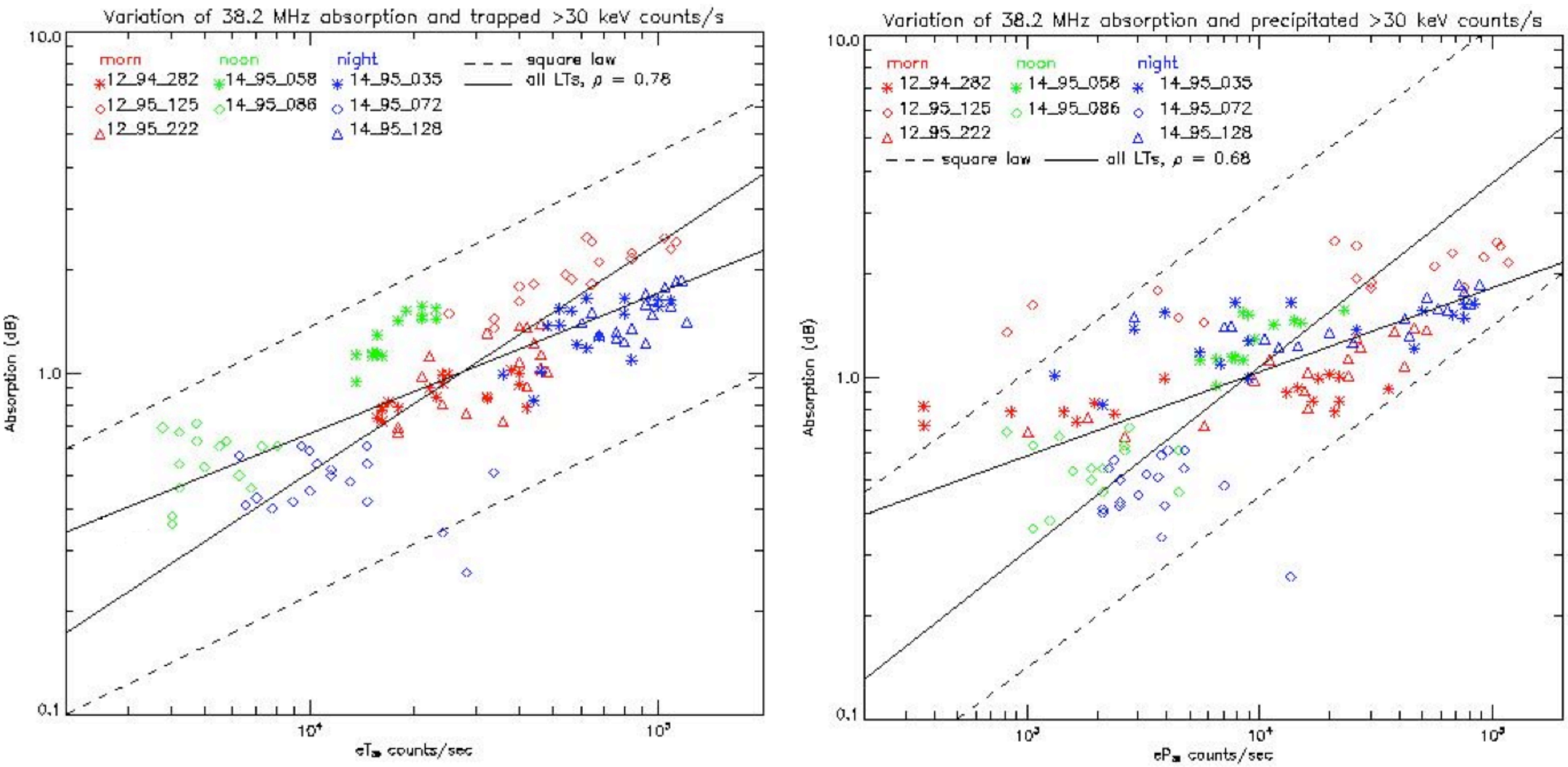

Figures 5 and 6: Variation of 38.2 MHz absorption with trapped and precipitated count rate (s^{-1}) for selected passes in the morning, noon and night sectors, showing individual passes colour-grouped in LT, regression lines for the population as a whole (solid lines), and square law 'rails' for comparison.

The regression lines and associated statistics over all local times are summarised in Table 2. Here the absorption is measured at 38.2 MHz and the flux is in units of $cm^{-2}s^{-1}sr^{-1}$, related to the count rate by flux ($cm^{-2}s^{-1}sr^{-1}$) = 100 x count-rate (s^{-1}). Since the correlation coefficients of absorption against the trapped and precipitated fluxes are not very different (0.78 and 0.68), these equations would be almost equally good as predictors of absorption from observed >30 keV flux, or of the flux from the measured radio absorption. A single prediction of absorption from the flux would be accurate within a factor of ≈ 1.4 in 70% of cases. A prediction of flux from absorption would be accurate to a factor of 2-3.

All Local Times	**Trapped flux (F_T)**	**Precipitated flux (F_P)**
Correl. Coeff.	0.78	0.68
Regression of y on x	y = 0.4118x – 2.649 ± 0.1358	y = 0.2454x – 1.458 ± 0.1611
Abs. in terms of flux	$A = 0.00224.F_T^{\ 0.4118}$	$A = 0.03483.F_P^{\ 0.2454}$
Standard error	Factor of 1.37	Factor of 1.45
Regression of x on y	x = 1.490y + 6.435 ± 0.2584	x = 1.860 + 5.944 ± 0.4435
Flux in terms of abs.	$F_T = 2.72.10^6.A^{1.49}$	$F_P = 8.79.10^5.A^{1.86}$
Standard error	factor of 1.79	factor of 2.78

Table 2: Summary of the statistics from Figures 5 and 6, showing the regression analysis between log(absorption) and log(30 keV flux) for both the trapped (F_T) and precipitated (F_P) populations. In the table, y = log[A(db)] and x = log(flux).

3. Pitch angle diffusion and its relation to spacecraft detector geometry and magnetic field orientation.

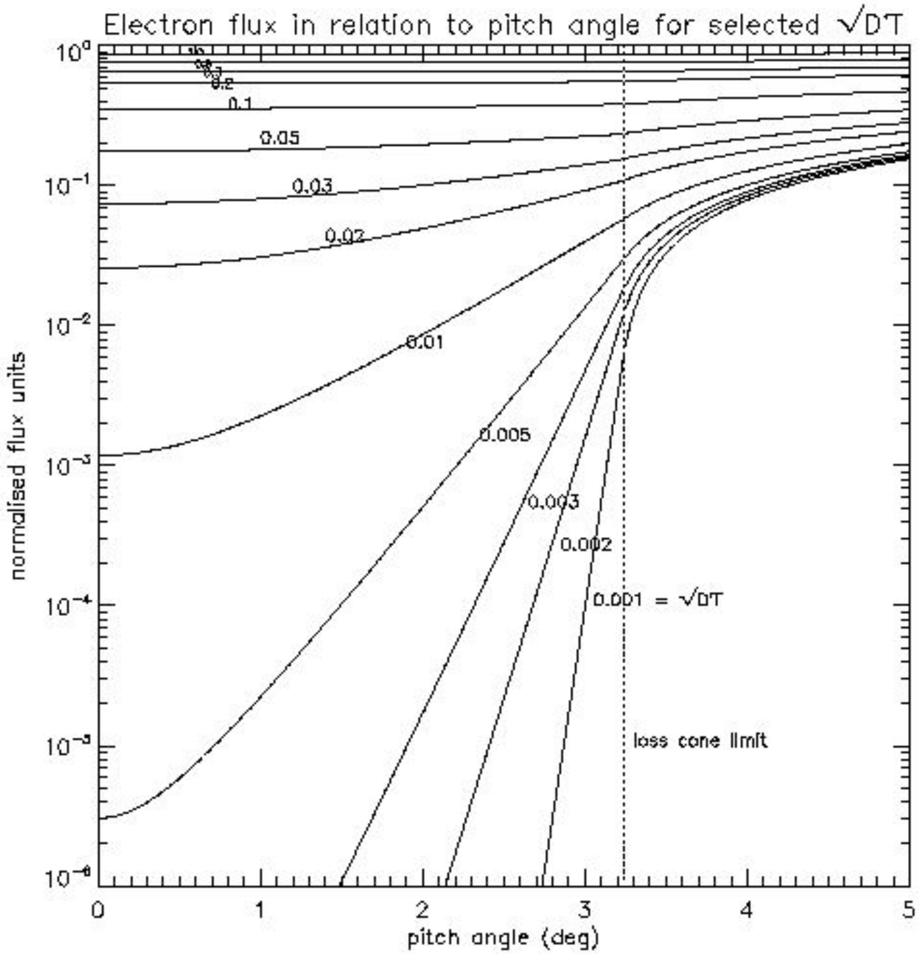

Figure 7: Electron flux against pitch angle for selected values of diffusion parameter.

Figure 7 shows the relative values of electron flux as a function of pitch angle and diffusion parameter √(D*T) according to the scattering theory of Kennel & Petschek (1966). The loss cone is assumed to be 3.24^{O} corresponding to the loss of electrons below 90 km in the atmosphere. The detector for precipitated electrons, however, covers pitch angles 2^{O} to 32^{O} at altitude 850 km, corresponding to 0.13^{O} to 2.04^{O} at the equator. Clearly, some particles will reach 90 km that were beyond the cone of the precipitated detector.

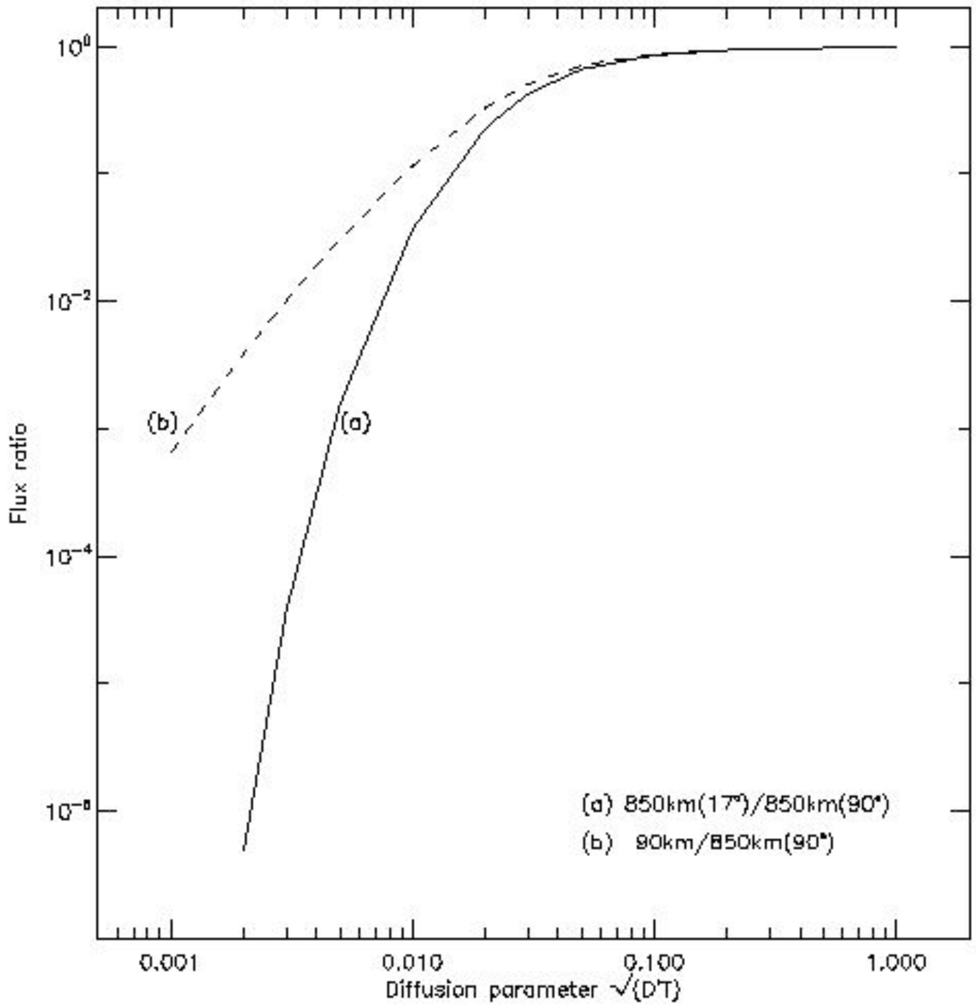

Figure 8: Calculated ratios between precipitated and trapped fluxes, and the flux reaching 90 km.

By integrating the flux across the respective detector cones and over a horizontal plane at 90 km (Figure 8) we can estimate how much the flux at 90 km will exceed that at the 0^{O} detector on the satellite, both in relation to the 90^{O} flux. This appears to explain part but not all of the observed anomaly in Figure 4.

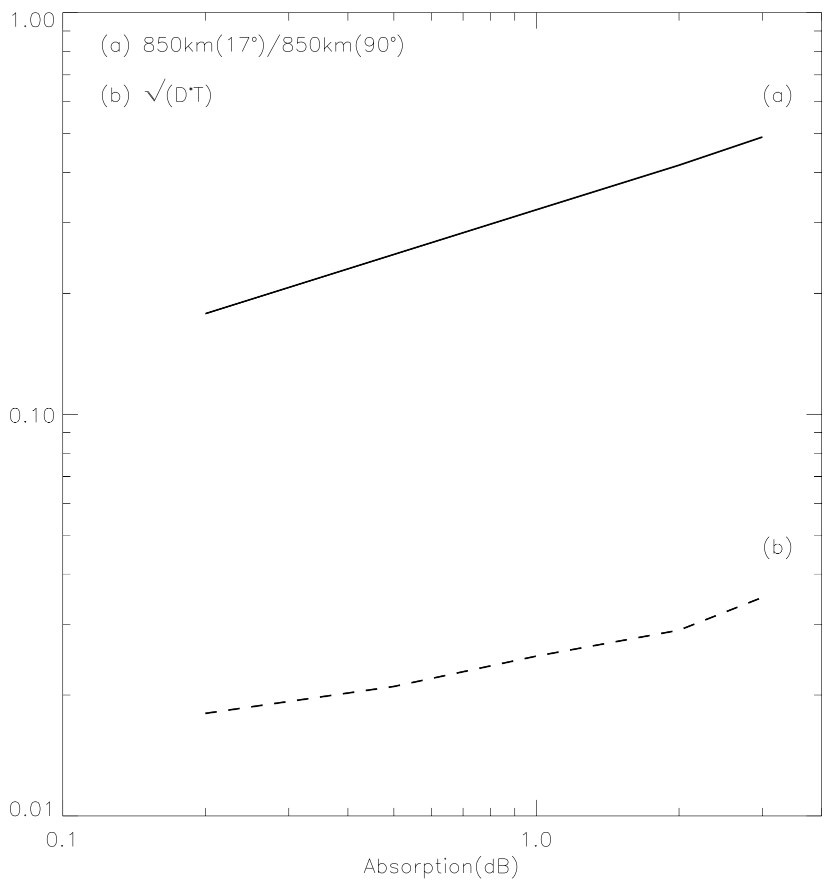

Figure 9: Estimates of (a) P/T and (b) √(D*T) against A(dB) at 38.2 MHz (narrow beam).

Curve 9(b) shows an estimate of the diffusion parameter √(D*T) as a function of the 38.2 MHz radio absorption observed at Kilpisjärvi. This uses the ratio F_P/F_T (curve 9(a)) taken from the observed relationships of Table 2, and the theoretical curve (a) of Figure 8.

The results may be compared with those derived by Collis et al. (1983) using particle observations at geosynchronous orbit and wide-beam riometer observations at 30 MHz. They reported strong scattering (F_P/F_T ≈ 1) for absorption greater than ≈ 6 dB, and diffusion parameter values of 0.014 and 0.0045 at 2 dB and 1 dB respectively.

Conclusions

1. The flux of >30 keV electrons observed on POES satellites at 850 km correlates well with the 38.2 MHz radio absorption measured with an imaging riometer at the ground.
2. It has been shown that the fine-scale fluctuations of particle flux are spatial rather than temporal.
3. The 'precipitated' flux tends to vary more than the 'trapped' flux, and the amount of variability depends strongly on the local time, being greatest in the morning sector.
4. Empirical relations have been derived between absorption and the electron fluxes which enable the absorption to be estimated from the flux to a factor of about 1.4, and the flux from the absorption to a factor of 2-3.
5. Computations suggest that a significant contribution to the absorption comes from electrons outside the reception cone of the 'precipitated' detector.
6. A relationship between the absorption and the diffusion parameter for >30 keV electrons has been derived.

Acknowledgment: We thank D.S. Evans of NOAA for providing the POES data.

References

Collis, P.N., Hargreaves, J.K., and Korth, A., *Loss cone fluxes and pitch angle diffusion at the equatorial plane during auroral radio absorption events*. J. Atmos. Terr. Phys., vol.45, pp. 231-243, 1983.

Kennel, C.F. and Petschek, H.E., *Limit on stably trapped particle fluxes*, J. Geophys. Res., vol.71, pp.1-28, 1966.